Measurement of charge carrier mobility in perovskite nanowire films by photo-celiv method

A. Aukštuolis, Mihaela Girtan, G.A. Mousdis, R. Mallet, M. Socol, M. Rasheed, A. Stanculescu

THE PUBLISHING HOUSE
OF THE ROMANIAN ACADEMY

PROCEEDINGS OF THE ROMANIAN ACADEMY, Series A,
Volume 18, Number 1/2017, pp. 34–41

MEASUREMENT OF CHARGE CARRIER MOBILITY IN PEROVSKITE NANOWIRE FILMS BY PHOTO-CELIV METHOD

Andrius AUKŠTUOLIS[1, 2], Mihaela GIRTAN[1], George A. MOUSDIS[3], Romain MALLET[4], Marcela SOCOL[5], Mohamed RASHEED[1], Anca STANCULESCU[5]

[1] Angers University, Photonics Laboratory (LPHIA), France
[2] Vilnius University, Faculty of Physics, Department of Solid State Electronics, Lithuania
[3] National Hellenic Foundation, Athens, Greece
[4] SCIAM, Angers University, France
[5] National Institute of Materials Physics, Bucharest, Magurele, Romania
Corresponding author: Mihaela GIRTAN, E-mail: mihaela.girtan@univ-angers.fr

Abstract. In this paper the holes' mobility for the configuration FTO/TiO_2/$CH_3NH_3PbI_3$/Spiro-MeOTAD/Au was measured for the first time by the Photo-CELIV method. The TiO_2 dense film was deposited by reactive sputtering at room temperature on FTO glass substrates. High crystalized perovskite films were deposited from solutions in one step by spin coating. Spiro-MeOTAD molecular glass was used as holes transporting layer. The highest holes' mobility from TiO_2 thin film through the perovskite and Spiro MeOTAD film to the top gold electrode was of order 8.5×10^{-7} cm^2/Vs.

Key words: perovskites, holes' mobility, photo-CELIV, solar cells, titanium oxide, $CH_3NH_3PbI_3$.

1. INTRODUCTION

The organic-inorganic perovskite solar cells have attracted much attention during the last five years and became the most promising material for the new generation of solar cells [1–5]. In particular, the organic-inorganic halide perovskites have several features such as: long charge carrier lifetime, long diffusion length and ambipolar charge transport capability, which made them very attractive materials for solar cells. Also their facile synthesis directly on the substrate at low temperature made them very suitable for applications on plastics substrates. Within the last six years the efficiencies of a typical solar cell: FTO/TiO_2dense/ TiO_2mes/Perovskite/HTM/Au rapidly increased from 4% to 21%.

However, despite the extremely fast progress, the materials' electronic properties that are crucial to the photovoltaic performance are relatively little understood. It is still under debate whether the photo-generated charges have an excitonic or a free-carrier character. Also, is not completely clear how the charge carriers' mobility of the active layer influences the overall performance and the origin of the high efficiencies of perovskite-based solar cell devices. Moreover the results strongly depend on the preparation method, the purity of the material and the film treatment, which can result to uncontrolled morphological variations and poor reproducibility of photovoltaic performance.

The theoretical calculations of mobility of charge carriers in hybrid perovskite, using the density functional theory including van der Waals interaction and the Boltzmann theory for diffusive transport in the relaxation time approximation, indicate that the mobility of electrons in MAPI perovskite crystals ranges from 5 to 10 $cm^2V^{-1}s^{-1}$ and that for holes within 1–5 $cm^2V^{-1}s^{-1}$, where the variations depend on the crystal structure investigated and the level of doping [6]. In the case of devices, the perovskite films are composed of microcrystals, or nanowires, hence the experimental values of mobility of charge carriers in perovskites films may differ from theoretical calculation by many orders of magnitude. On the other side the charge carrier's mobility in the Spiro-Me-O-TaD holes transporter layer is much lower, which can globally conduct to a lower charge carrier's mobility through the whole device multilayer structure.

In this paper we investigate the mobility of holes through the interface $CH_3NH_3PbI_3$/Spiro-MeOTAD by using the Photo-generated Charge Extraction by Linearly Increasing Voltage (Photo-CELIV) method. Photo-CELIV is a new and powerful technique for studying charge transport physics, particularly in disordered systems such as organic semiconductors [7]. We considered here the multi-layer structure based on methyl-ammonium lead-iodide perovskite: FTO/TiO_2/$CH_3NH_3PbI_3$/Spiro-MeOTAD/Au.

The TiO_2 film may be deposited by different methods such as spin coating [8–9], spray pyrolysis [10-13], and PLD [14–16]. Different from the most common studied system using MAPI perovskite, in this study the TiO_2 dense film was deposited by sputtering and not by spray pyrolysis. The advantage of sputtering method comparing to spray pyrolysis is the very high reproducibility and deposition at room temperature. There is no need to heat the substrate FTO/glass films. In our previous studies [17–33] we have demonstrated that heating of transparent conducting electrodes at more than 300 °C conduct to irreversible changes of the electrical properties.

2. EXPERIMENTAL SETTING

The configuration of studied samples is described in Fig.1. Commercial FTO covered glasses were used as transparent electrodes. A dense titanium oxide (TiO_2) film of 30 nm was deposited by reactive sputtering using a metallic titanium target in oxygen atmosphere. Two equimolar solutions of 0.1983 g (1.25 mmole) CH_3NH_3I at 0.25 ml dry DMF 0.5785 g (1.25 mmole) PbI_2 at 25 ml dry DMF, were mixed, just before the spin coating. The CH_3NH_3I was prepared as follows: 20 ml of a methylamine solution (Ferak 40/% w/v) containing 8 g methylamine (257 mmol) was diluted with 80 ml of ethanol. To this solution a Hydroiodic acid solution in water (Merck 57 % w/v) was added slowly under stirring until the PH of solution turns to acidic (about 60 ml). The solution was stirred for 2 h at room temperature and evaporated to dryness. The solid was dispersed to anhydrous diethylether and filtrated. It washed copiously with anhydrous diethylether to obtain white crystals. The CH_3NH_3I crystals were dried at 60 ^{0}C in a vacuum oven overnight. The PbI_2 was prepared as follows: 3.3 g (10 mmol) of $Pb(NO_3)_2$ (Serva anal. Grade) were diluted to 50 ml of distilled water. To this solution, a solution of 3.3 g (20 mmol) of KI (Merck Reag. Ph. Eur.) in 50 ml distilled water was added under stirring, slowly at room temperature. The gold-yellow precipitate was filtered and recrystallized from water to give golden-yellow crystals. The PbI_2 crystals were dried at 60 ^{0}C in a vacuum oven overnight. The perovskite film was prepared, in one step, by spin coating. The solution was spin on the top of TiO_2 dense film at 1 600 RPM during 30 s. For the Hole Transporting Material (HTM) thin films preparation was used the Spiro-MeOTAD purchased from MERCK. A solution of (75 mg in 0.3 ml CB) was spin coat at 3 500 RPM during 20 s. The top gold electrode (of about 40 nm) was deposited by sputtering under vacuum.

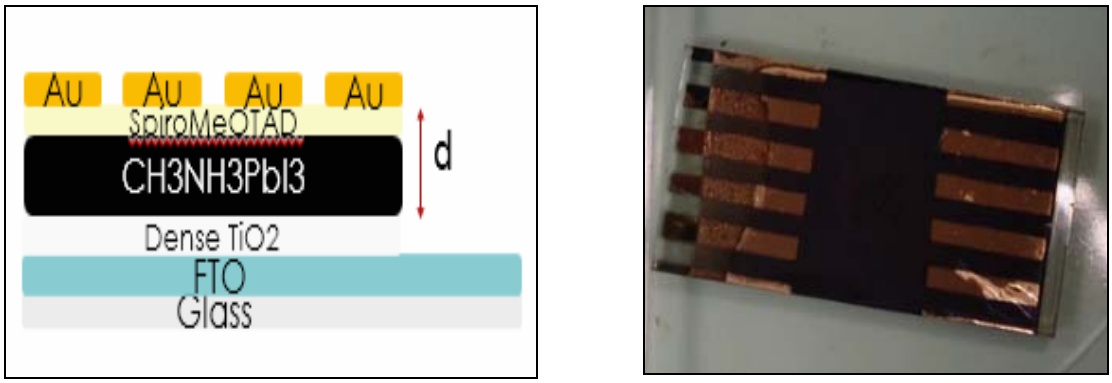

a) b)

Fig. 1 – a) Multi-layer solar cells perovskite configuration; b) sample photo.

The principle of charge carriers' mobility measurements by Photo-CELIV method is described briefly in Fig. 2.

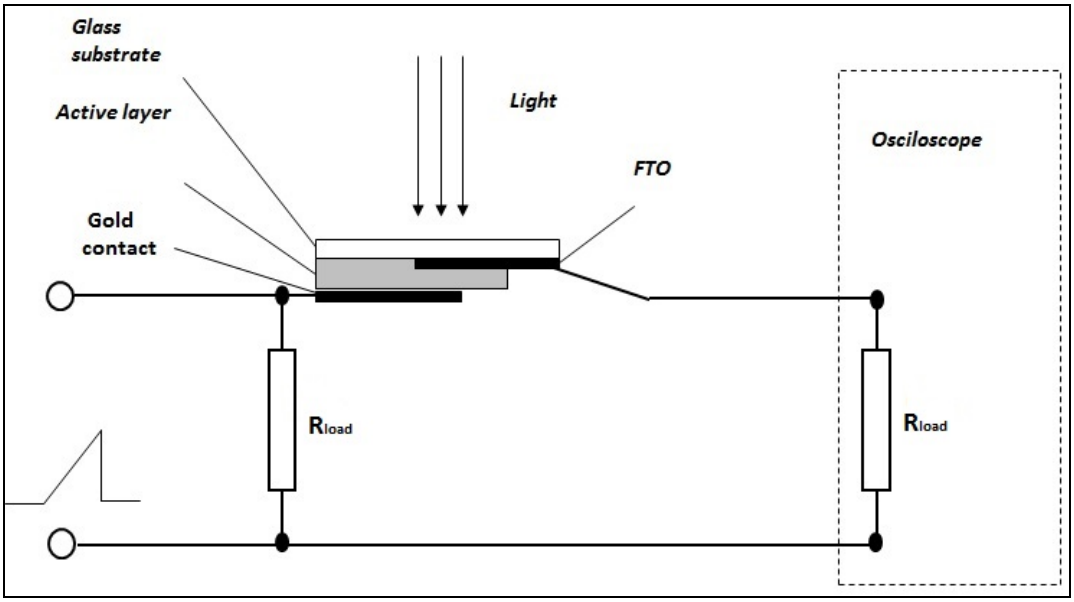

Fig. 2 – Photo-CELIV setup.

The method is based on the analysis of the extraction of photo-generated charge carriers current transients when a ramp voltage pulse is applied to a sample with a blocking contact (Fig. 3). The time t_{max} corresponding to the maximal current density depends on the mobility of charge carriers (μ). The initial slope of the current density transient depends on the bulk conductivity, σ, of the sample. The concentration of photo-generated charge carriers Δn or Δp can be estimated by integration of the extracted part of current density transients (above $j(0)$). So the carriers' concentration and the mobility of equilibrium charge carriers may be estimated independently. A short laser pulse ($\lambda = 532$ nm) of 250 ms is applied before starting the current density measurement (moment $t = 0$ see Fig. 3). This short light pulse will create more charge carriers and we will call j_{light} the density of current after the exposure of the sample to this short light pulse. j_{dark} is the current density measured in the absence of the light pulse (in dark). The density of photo-generated current, $j_{photogen}$ is given by the difference between j_{light} and j_{dark}: $j_{photogen} = j_{light} - j_{dark}$.

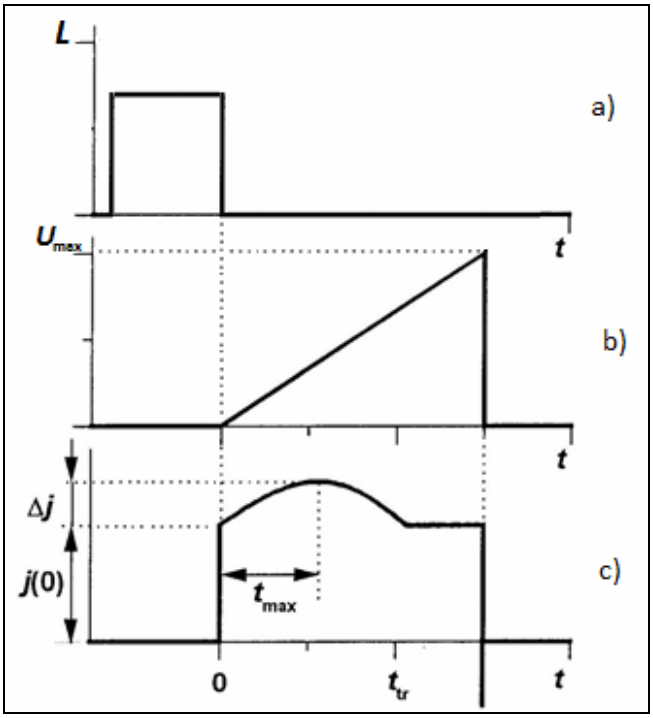

Fig. 3. – Schematic illustration of CELIV a) light pulse; b) ramp voltage pulse applied to sample; c) current density in the sample after ramp voltage is applied [12].

By varying A – the voltage slope, the best conditions can be achieved to get the initial step $j(0)$.

In the case of samples with low electrical conductivities, the extracted charge carriers do not significantly affect the electric field inside the samples and the charge carriers mobility can be calculated easily using the following formula:

$$t_{\max} = \sqrt{\frac{2d^2}{3\mu A}} \quad . \tag{1}$$

If the electrical conductivity of the samples is high, then the mobility can be calculated by the formula:

$$t_{\max} = \sqrt[3]{\frac{3\tau_\sigma d^2}{\mu A}}. \quad (2)$$

Here τ_σ is Maxwell's relaxation time. In most of the cases, τ_σ could be determined from the period of time between the moment of the signal start and the moment when the current density transient reaches the double initial step value: $2j(0)$.

In this paper the mobility of holes through the perovskite and Spiro MeOTAD film was determined. The thickness (d), corresponding to this transversal region (see Fig. 1) was determined by profilometry and was 1.2 μm. The value of $t_{\max}$ was determined from the graph of photogenerated current density.

3. RESULTS AND DISCUSSIONS

Figure 4b–c depicts the SEM micrographs for the methylamonium-lead triodine (MAPI) thin films deposited on glass. As one can see the prepared perovskite films presented long crystals (more than 200 μm). Several studies have established that halide perovskite exhibits unusually long diffusion excitons lengths reaching over 100 nm. This could be explained for the extremely long dimension of these perovskite crystals. Figure 4d presents the SEM micrograph of top Spiro-MeOTAD layer deposited on nanowires perovskite film.

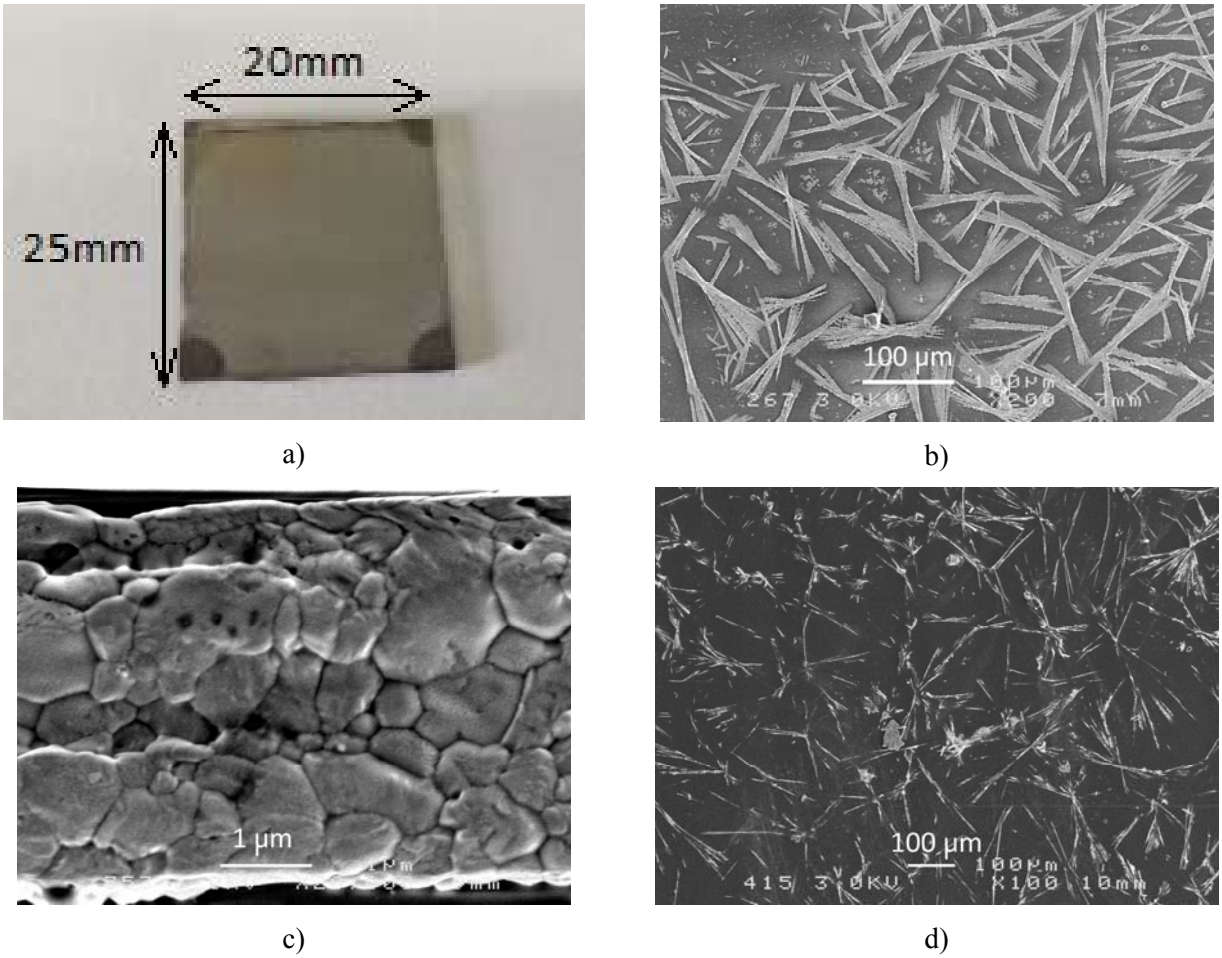

a) b)

c) d)

Fig. 4 – Perovskite nanowire film on glass substrate: a) sample photo; b), c), SEM micrograph of films deposited on glass substrates; d) top view after Spiro-MeOTAD film deposition.

The XRD analysis for the perovskite films deposited on glass, FTO, and TiO_2 films, respectively, are given in Fig. 5.

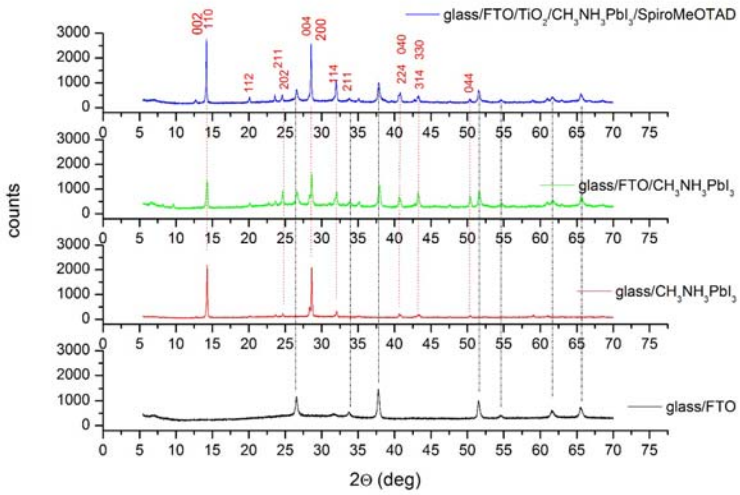

Fig. 5 – XRD spectra for MAPI thin films deposited on glass, FTO/glass, and TiO_2 dense films, respectively. The XRD spectra of the reference FTO/glass is also given.

It was found through powdered X-ray diffraction (XRD) that the methylammonium lead iodide ($MAPbI_3$) perovskite exists in the cubic Pm3m phase at high temperature above 330 K, below which it undergoes a phase transition to the tetragonal I4/mcm phase and then to the orthorhombic Pnma phase below 170 K [34]. There are no critical differences between the tetragonal and cubic phases, except a slight rotation of PbI_6 octahedra along the *c*-axis and a small difference in energy. The XRD spectra of the cubic and tetragonal phases are similar with slight differences that consist mainly from splitting of the peaks 100 and 200 of cubic phase to the 002, 110 and 004, 220 of the tetragonal phase, respectively. Moreover two new peaks (211) and (213) appear in the tetragonal phase. The most safe criterion of XRD spectra to distinguish between them is the minor diffraction from the (211) planes at $2\theta \sim 23.5°$.

In our case the presence of a peak at 23.68° in the XRD spectra indicates the presence of the tetragonal I4/mcm phase. The peak at $2\theta = 14.29°$ can be deconvoluted [35] into two peak components at 14.14° and 14.29° attributed to the 002 and 110 diffractions, respectively.

The X-ray diffraction patterns of $CH_3NH_3PbI_3$ films on different substrates (glass, FTO, and TiO_2) confirm the tetragonal 3D structure and the space group I4/mcm. No peaks of PbI_2 are observed indicating that is no excess of PI2 and the reaction of perovskite formation was completed. The peaks intensity increase in the case of the deposition of perovskite film on TiO_2 dense films indicating a better crystallisation comparing to films deposited on FTO or glass. The crystallite size influences the transport of charge carriers. A better crystallization and large crystalline size are favourable to a higher transport of charge carriers.

In Fig. 6 is given the current density J_{light} after laser pulse excitation. From this graph the value of τ_σ could be extracted.

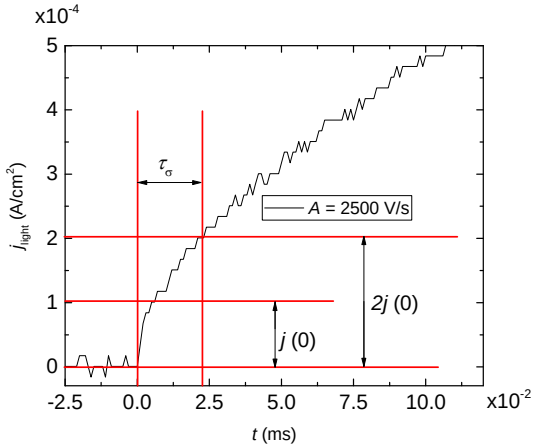

Fig. 6 – The light current density; τ_σ is Maxwell's relaxation time.

The value of t_{max} was determined from the maximum of the photo-generated current (see Fig.7).

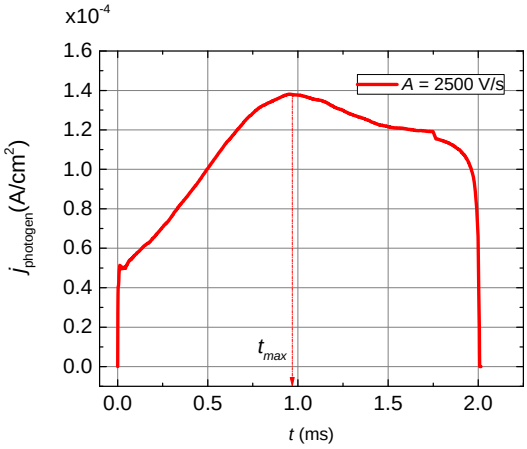

Fig. 7 – The photo-generated current density.

The form of current density kinetics suggests that the investigated layers were highly conductive. Hence, from the values of τ_σ and t_{max} the holes mobility μ_h was calculated according to eq. (2):

$$\mu_h = \frac{3\tau_\sigma d^2}{A t_{\max}^{\ 3}}. \tag{3}$$

The obtained values for different slopes of increasing voltage are given in Table 1. This mobility corresponds to the charge transport between the TiO_2 interface and top gold contact.

The experimental values of Spiro-OMeTAD, one of the hole transporting material (HTM) with the highest hole mobility, is of about 4×10^{-5} $cm^2V^{-1}s^{-1}$ [36].

The high reported values of the holes mobility correspond only to theoretical calculation for $CH_3NH_3PbI_3$ nanocrystals. In practical cases the measured values of mobility of holes are much smaller, of order of 10^{-5} $cm^2V^{-1}s^{-1}$ and this could be explained by the disorder and grain boundaries in the case of polycrystalline films, or due to the interfaces between the perovskite nanowires and Spiro-MeOTAD molecular glass material in this case.

Table 1

The calculated values of holes' mobility
in $CH_3NH_3PbI_3$/Spiro-MeOTAD thin film by using Photo-CELIV

U_{max} (V)	t_{ramp} (s)	ramp A (V/s)	τ_σ (s)	$t_{\max}$ (s)	μ_h (cm^2/Vs)
5	2×10^{-3}	2 500	2.2×10^{-5}	9.6×10^{-4}	5.2×10^{-7}
5	1×10^{-3}	5 000	2.0×10^{-5}	6.3×10^{-4}	8.0×10^{-7}
5	0.5×10^{-3}	10 000	1.3×10^{-5}	4.3×10^{-4}	8.5×10^{-7}

4. CONCLUSIONS

The mobility of holes for the configuration FTO/TiO2/CH3NH3PbI3/Spiro-MeOTAD/Au was measured by the Photo-CELIV method. Structural and morphological properties was analysed by X-ray diffraction and Scanning Electron Microscopy. The holes' mobility was determined by photo-CELIV method using a green laser (λ = 532 nm). The highest holes' mobility from TiO2 thin film through the perovskite and Spiro MeOTAD film to the top gold electrode was of order 8.5×10^{-7} cm^2/Vs. The electrical properties were correlated with the morphological and structural properties of the perovskite film.

ACKNOWLEDGEMENTS

One of the authors (G.A. Mousdis) would like to acknowledge the financial support from the Hellenic General Secretariat for Research and Technology through project Polynano-Kripis 447963.

REFERENCES

1. M. GRATZEL, *The light and shade of perovskite solar cells*, Nat. Mater., **13**, *9*, pp. 838–842, 2014.
2. M.A. GREEN, A. HO-BAILLIE, H.J. SNAITH, *The emergence of perovskite solar cells*, Nat. Photonics, **8**, *7*, pp. 506–514, 2014.
3. H.J. SNAITH, *Perovskites: The Emergence of a New Era for Low-Cost, High-Efficiency Solar Cells*, J. Phys. Chem. Lett., **4**, *21*, pp. 3623–3630, 2013.
4. N.G. PARK, *Organometal Perovskite Light Absorbers Toward a 20% Efficiency Low-Cost Solid-State Mesoscopic Solar Cell*, J. Phys. Chem. Lett., **4**, *15*, pp. 2423–2429, 2013.
5. Q.F. DONG, Y.J. FANG, Y.C. SHAO, P. MULLIGAN, J. QIU, L. CAO, J.S. HUANG, *Electron-hole diffusion lengths > 175 mu m in solution-grown $CH_3NH_3PbI_3$ single crystals*, Science, **347**, *6225*, pp. 967–970, 2015.
6. CARLO MOTTA, FEDWA EL-MELLOUHI, STEFANO SANVITO, *Charge carrier mobility in hybrid halide perovskites*, Scientific Reports, **5**, *12746*, 2015.
7. N. NEKRAŠAS, K. GENEVIČIUS, M. VILIŪNAS, G. JUŠKA, *Features of current transients of photogenerated charge carriers, extracted by linearly increased voltage*, Chemical Physics, **404**, pp. 56–59, 2012.
8. N. IFTIMIE, D. LUCA, F. LACOMI, M. GIRTAN, D. MARDARE, *Gas sensing materials based on TiO_2 thin films*, J. Vac. Sci. Amp Technol. B, **27**, *1*, pp. 538–541, 2009.
9. A.V. MANOLE, M. DOBROMIR, M. GIRTAN, R. MALLET, G. RUSU, D. LUCA, *Optical properties of Nb-doped TiO_2 thin films prepared by sol-gel method*, Ceram. Int., **39**, *5*, pp. 4771–4776, 2013.
10. I. VAICIULIS, M. GIRTAN, A. STANCULESCU, L. LEONTIE, F. HABELHAMES, S. ANTOHE, *On titanium oxide spray deposited thin films for solar cells applications*, Proc. Romanian Acad. A, **13**, *4*, pp. 335–342, 2012.
11. C. ADOMNITEI, D. LUCA, M. GIRTAN, I. SANDU, V. NICA, A.V. SANDU, D. MARDARE, *Nb-doped TiO_2 thin films deposited by spray pyrolysis method*, J. Optoelectron. Adv. Mater., **15**, *5–6*, pp. 519–522, 2013.
12. D. MARDARE, F. IACOMI, N. CORNEI, M. GIRTAN, D. LUCA, *Undoped and Cr-doped TiO_2 thin films obtained by spray pyrolysis*, Thin Solid Films, **518**, *16*, pp. 4586–4589, 2010.
13. D. CHAPRON, M. GIRTAN, J.Y. LE POMMELEC, A. BOUTEVILLE, *Droplet dispersion calculations for ultrasonic spray pyrolysis depositions*, J. Optoelectron. Adv. Mater., **9**, *4*, pp. 902–906, 2007.
14. A. STANCULESCU, M. SOCOL, G. SOCOL, I.N. MIHAILESCU, M. GIRTAN, F. STANCULESCU, *Maple prepared organic heterostructures for photovoltaic applications*, Appl. Phys. -Mater. Sci. Process., **104**, *3*, pp. 921–928, 2011.
15. F. STANCULESCU, O. RASOGA, A.M. CATARGIU, L. VACAREANU, M. SOCOL, C. BREAZU, N. PREDA, G. SOCOL, A. STANCULESCU, *MAPLE prepared heterostructures with arylene based polymer active layer for photovoltaic applications*, Appl. Surf. Sci., **336**, pp. 240–248, 2015.
16. A. STANCULESCU, L. VACAREANU, M. GRIGORAS, M. SOCOL, G. SOCOL, F. STANCULESCU, N. PREDA, E. MATEI, I. IONITA, M. GIRTAN, I.N. MIHAILESCU, *Thin films of arylenevinylene oligomers prepared by MAPLE for applications in non-linear optics*, Appl. Surf. Sci., **257**, *12*, pp. 5298–5302, 2011.
17. S. IFTIMIE, R. MALLET, J. MERIGEON, L. ION, M. GIRTAN, S. ANTOHE, *On the structural, morphological and optical properties of ITO, ZnO, ZnO: Al and NiO thin films obtained by thermal oxidation*, Dig. J. Nanomater. Biostructures, **10**, *1*, pp. 221–229, 2015.
18. M. GIRTAN, A. BOUTEVILLE, G.G. RUSU, M. RUSU, *Preparation and properties of SnO_2: F thin films*, J. Optoelectron. Adv. Mater., **8**, *1*, pp. 27–30, 2006.
19. M. GIRTAN, R. MALLET, *On the electrical properties of transparent electrodes*, Proc. Romanian Acad. A, **15**, *2*, pp. 146–150, 2014.
20. F.Z. GHOMRANI, S. IFTIMIE, N. GABOUZE, A. SERIER, M. SOCOL, A. STANCULESCU, F. SANCHEZ, S. ANTOHE, M. GIRTAN, *Influence of Al doping agents nature on the physical properties of Al:ZnO films deposited by spin-coating technique*, Optoelectron. Adv. Mater.-Rapid Commun., **5**, *3–4*, pp. 247–251, 2011.
21. M. RUSU, G.G. RUSU, M. GIRTAN, S.D. SEIGNON, *Structural and optical properties of ZnO thin films deposited onto ITO/glass substrates*, J. Non-Cryst. Solids, **354**, *35–39*, pp. 4461–4464, 2008.
22. M. GIRTAN, *Investigations on the optical constants of indium oxide thin films prepared by ultrasonic spray pyrolysis*, Mater. Sci. Eng. B-Solid State Mater. Adv. Technol., **118**, *1–3*, pp. 175–178, 2005.
23. M. GIRTAN, A. VLAD, R. MALLET, M.A. BODEA, J.D. PEDARNIG, A. STANCULESCU, D. MARDARE, L. LEONTIE, S. ANTOHE, *On the properties of aluminium doped zinc oxide thin films deposited on plastic substrates from ceramic targets*, Appl. Surf. Sci., **274**, pp. 306–313, 2013.
24. M. GIRTAN, G.G. RUSU, S. DABOS-SEIGNON, M. RUSU, *Structural and electrical properties of zinc oxides thin films prepared by thermal oxidation*, Appl. Surf. Sci., **254**, *13*, pp. 4179–4185, 2008.
25. G.G. RUSU, M. GIRTAN, M. RUSU, *Preparation and characterization of ZnO thin films prepared by thermal oxidation of evaporated Zn thin films*, Superlattices Microstruct., **42**, 1–*6*, pp. 116–122, 2007.
26. M. GIRTAN, *The influence of post-annealing treatment on the electrical properties of In_2O_3 thin films prepared by an ultrasonic spray CVD process*, Surf. Coat. Technol., **184**, *2–3*, pp. 219–224, 2004.
27. M. GIRTAN, G. FOLCHER, *Structural and optical properties of indium oxide thin films prepared by an ultrasonic spray CVD process*, Surf. Coat. Technol., **172**, *2–3*, pp. 242–250, 2003.
28. M. GIRTAN, H. CACHET, G. I. RUSU, *On the physical properties of indium oxide thin films deposited by pyrosol in comparison with films deposited by pneumatic spray pyrolysis*, Thin Solid Films, **427**, *1–2*, pp. 406–410, 2003.
29. M. GIRTAN, G.I. RUSU, G.G. RUSU, *The influence of preparation conditions on the electrical and optical properties of oxidized indium thin films*, Mater. Sci. Eng. B-Solid State Mater. Adv. Technol., **76**, *2*, pp. 156–160, 2000.
30. M. GIRTAN, G.I. RUSU, G.G. RUSU, S. GURLUI, *Influence of oxidation conditions on the properties of indium oxide thin films*, Appl. Surf. Sci., **162**, pp. 492–498, 2000.

31. M. GIRTAN, M. SOCOL, B. PATTIER, M. SYLLA, A. STANCULESCU, *On the structural, morphological, optical and electrical properties of sol-gel deposited ZnO In films*, Thin Solid Films, **519**, *2*, pp. 573–577, 2010.
32. M. GIRTAN, R. MALLET, D. CAILLOU, G.G. RUSU, M. RUSU, *Thermal stability of poly(3,4-ethylenedioxythiophene)-polystyrenesulfonic acid films electrical properties*, Superlattices Microstruct., **46**, *1–2*, pp. 44–51, 2009.
33. M. GIRTAN, M. KOMPITSAS, R. MALLET, I. FASAKI, *On physical properties of undoped and Al and In doped zinc oxide films deposited on PET substrates by reactive pulsed laser deposition*, Eur. Phys. J.-Appl. Phys., **51**, *3*, 2010.
34. T. BAIKIE, Y. FANG, J.M. KADRO, M. SCHREYER, F. WEI, S.G. MHAISALKAR, M. GRAETZEL, T.J. WHITE, *Synthesis and Crystal Chemistry of the Hybrid Perovskite $(CH_3NH_3)PbI_3$ for Solid-State Sensitised Solar Cell Applications*, J. Mater. Chem. A, **18**, *1*, pp. 5628–5641, 2013.
35. ZHAONING SONG, SUNETH C. WATTHAGE, ADAM B. PHILLIPS, BRANDON L. TOMPKINS, RANDY J. ELLINGSON, MICHAEL J. HEBEN., *Impact of Processing Temperature and Composition on the Formation of Methylammonium Lead Iodide Perovskites*, Chem. Mater., **27**, *13*, pp. 4612–4619, 2015.
36. TOMAS LEIJTENS, I-KANG DING, TOMMASO GIOVENZANA, JASON T. BLOKING, MICHAEL D. MCGEHEE, ALAN SELLINGER, *Hole Transport Materials with Low Glass Transition Temperatures and High Solubility for Application in Solid-State Dye-Sensitized Solar Cells*, ACS Nano, **6**, *2*, pp.1455–1462, 2012.

Received June 17, 2016